Inhibition of overactive TGF-β signaling by prostacyclin analogues in pulmonary arterial hypertension (PAH)

Takeshi Ogo, H. M. Chowdhury, Jun Yang, Lu Long, Xiaohui Li, Yamila N. Torres Cleuren, Nicholas W Morrell, Ralph T. Schermuly, Richard C. Trembath and Md. Talat Nasim

From the Departments of Medical and Molecular Genetics (T.O., H.M.C., R.C.T., M.T.N.), King's College London, United Kingdom; (T.O.) Department of Pulmonary Circulation, Division of Cardiology, National Cerebral and Cardiovascular Center Hospital, Osaka, Japan; Division of Respiratory Medicine, Department of Medicine (N.W.M., L.L., X.L. and J.Y.), University of Cambridge School of Clinical Medicine, United Kingdom; Department of Internal Medicine (R.T.S.), Justus-Liebig-University, Giessen, Germany.

Address correspondence to Dr. T. Nasim at the Division of Genetics and Molecular Medicine, King's College London, School of Medicine, Tower Wing, Guy's Hospital, Great Maze Pond, London SE1 9RT, United Kingdom
E-mail: talat.nasim@kcl.ac.uk
Tel: +44 (0) 20-718-89505, Fax: +44 (0) 20-7188-2585

Abstract

Heterozygous loss of function mutations in the type II bone morphogenetic protein receptor (BMPR-II), a member of the transforming growth factor (TGF-β) receptor family, underlie the majority of familial cases of pulmonary arterial hypertension (PAH). The TGF-β1 pathway is activated in PAH and inhibitors of TGF-β1 signaling prevent the development and progression of PAH in experimental models. However, the effect of currently utilized therapies on the TGF-β pathway is not known.
Prostacyclin analogues remain the first line of treatment for clinical PAH. We hypothesized that these agents effectively decrease the activity of the TGF-β1 pathway. Beraprost sodium (BPS), a prostacyclin analogue selectively inhibits proliferation in a dose-dependent manner in mouse primary pulmonary arterial smooth muscle cells (PASMCs) harbouring a pathogenic *BMPR2* nonsense mutation in both the presence and absence of TGF-β1 stimulation. This study demonstrates that this agent inhibits TGF-β1–induced SMAD-dependent and -independent signaling via a PKA dependent pathway by reducing the phosphorylation of SMADs 2 and 3 and p38MAPK proteins. Finally, in a monocrotaline (MCT)-induced rat model of PAH, which is associated with increased TGF-β signaling, this study confirms that treprostinil (TPS), a stable prostacyclin analogue, inhibits the TGF-β pathway by reducing SMAD3 phosphorylation. Taken together, these data suggest that prostacyclin analogues inhibit dysregulated TGF-β signaling *in vitro* and *in vivo* and reduce BMPR-II-mediated proliferation defects in mutant mice PASMCs.

Key words

PAH, *BMPR2*, TGF-β signaling, prostacyclins and PASMC

Introduction

Pulmonary arterial hypertension (PAH) is a devastating cardiovascular disorder caused by extensive vascular remodeling of blood vessels in the lung and in the absence of effective therapy, leads to right-heart failure and death. The major features of this disorder include increased resistance in the small pulmonary arteries and vascular remodeling due to abnormal proliferation of endothelial and pulmonary arterial smooth muscle cells (PASMCs). Loss-of-function mutations in the type II bone morphogenetic protein receptor (BMPR-II), a member of the transforming growth factor-β (TGF-β) superfamily, underlie the majority (>80%) of cases of familial PAH (1), (2), identified an important role for TGF-β signaling in the development of PAH.

Bone morphogenetic proteins (BMPs) are members of the TGF-β superfamily of cytokines required for cellular differentiation and mammalian development. Activation of the receptor complex by ligand stimulation generates a phosphorylation relay of cytoplasmic signaling proteins, including the SMAD family capable of transducing the downstream signaling pathways. BMPs signal through a specific set of regulatory SMADs namely SMAD 1, 5 and 9, whilst TGF-β-mediated signaling occurs via SMAD2/3 proteins. On activation, these regulatory SMADs translocate to the nucleus in complex with co-SMAD (SMAD4) to directly regulate gene transcription (3). BMPs and TGF-β have also been reported to activate SMAD independent signaling including ERK, JNK and p38MAPK (4), (5-9).

To gain further insight as to the pathogenesis of PAH, we and others have investigated the functional consequences of *BMPR2* mutation. In cell-based studies, mutations in the *BMPR2* gene have been shown to disrupt the BMP-induced SMAD1/5 pathway (10), (11). In animal models, mice deficient in BMPR-II (p.R899X) showed increased susceptibility to pulmonary hypertension and vascular remodeling, suggesting a link between dysfunctional BMPR-II signaling and PAH (8). In addition, an increasing number of studies suggest the involvement of TGF-β signaling in PAH. *In vitro*, TGF-β1 elicits a pro-proliferative response in PASMCs isolated from PAH patients (PAH-PASMCs) compared to controls (12). Elevated TGF-β signaling has been implicated in a number of preclinical PAH models, including the aorto-pulmonary shunt model in lambs (13), hypoxia-induced PAH in mice and the monocrotaline (MCT)-induced model in rats (14). In addition, phosphorylation of SMAD2, a cytoplasmic signaling protein downstream of the TGF-β receptor 1 (ALK 5), is increased in plexiform lesions from PAH patients (15). Taken together, these data suggest a role for activated TGF-β signaling in the pathogenesis of PAH and present the potential of targeting this pathway in PAH for therapeutic intervention (16). However, the molecular mechanisms by which TGF-β signaling is activated consequent to impaired BMPR-II signaling have not been investigated and the impact of current therapies on these pathways remains unknown.

Prostacyclin therapy has significant beneficial effects in patients with severe PAH, and this has been examined in an experimental animal model and human PASMCs. In the monocrotaline-induced rat model, administration of beraprost sodium (BPS) significantly improved PAH, right ventricular hypertrophy, and pulmonary medial thickness without any adverse effects (17). Prostacyclin analogues have also been shown to inhibit serum/PDGF-induced PASMC proliferation via a cyclic adenosine monophosphate (cAMP)-dependent pathway (18). In fibroblasts and the skin of scleroderma patients, iloprost has been shown to suppress TGF-β–induced expression of collagen and connective tissue growth factor (CTGF) genes via PKA-dependent mitogen activated protein kinase (MAPK) pathways (19), (20), suggesting a potential interaction between prostanoids and TGF-β signaling. The involvement of activated TGF-β

signaling in the pathogenesis of PAH led us to hypothesize that prostacyclin analogues may also inhibit activated TGF-β signaling in PAH.

In this report, we investigate the beneficial effects of prostacyclin analogues on proliferation and TGF-β signaling in mouse primary PASMCs harbouring a pathogenic nonsense mutation in the *BMPR2* gene. We show that prostacyclin analogues inhibit the pro-proliferative phenotype in both the presence and absence of TGF-β1 stimulation. Furthermore, we observe that prostanoids inhibit TGF-β1–induced SMAD-dependent and -independent MAPK pathways by reducing the phosphorylation of SMAD3 and p38 MAPK proteins. Finally, we demonstrate that prostacyclin analogues inhibit the overactive TGF-β pathway in the monocrotaline-induced PAH rat model.

Materials and Methods

Supporting Information contains full experimental details.

Cell culture, transient transfection, enzymatic assay and western blots
Cell culture and transfections were carried out as described elsewhere (21), (22). Mouse PASMCs were derived from wild type (*bmpr2*$^{+/+}$) and knock-in mice (*bmpr2* $^{R899X+/-}$) harbouring a disease-associated nonsense mutation (p.R899X) in the *bmpr*2 gene. Luciferase and β-galactosidase activities were determined with the Dual-light Reporter Assay systems (Applied Biosystems) using an ORION-II Plate Luminometer (Berthold) according to manufacturers protocols. SMAD-responsive reporter assay in mammalian cells was performed as previously described (21). Western blots were carried out using anti-phospho specific p38MAPK (Thr180/Thr182), SMAD2 (Ser245/250/255) and SMAD3 (Ser463/465) (Cell Signaling) antibodies following manufacturer's protocols. To confirm equal loading the membranes were stripped and re-probed with anti-β-actin antibody (Cell Signaling).

Quantification of proliferation and cyclic AMP (c-AMP) production of mouse primary PASMCs
To determine proliferation, PASMCs were seeded at 0.2X10 ^{5} per well in a clear 96 well plate in DMEM containing 10% FBS. After 24 hours, the medium was replaced by either fresh DMEM/0.1% FBS alone or containing TGF-β1 (10ng/ml) (R&D Systems), SD208 (10μM) (TOCRIS), SB203580 (0.1-10 μM) (TOCRIS), or BPS (0.5-20 μM) (Cayman Chemicals) for 3-4 days. Cell proliferation was determined using CellTiter 96® Aq_{ueous} One Solution Cell Proliferation Assay (Promega) following the manufacturer's protocol. Absorbance was recorded at 490nm using Omega Plate Reader (BMG Labtech). Production of cAMP was determined using the luminescence-based cAMP-Glo ™ Assay kit (Promega) following the manufacturer's protocol. Luminescence was determined using ORION-II plate Luminometer (Berthold).

The monocrotaline induced PAH rat Model

Male Sprague-Dawley rats (Charles River, Sulzfeld, Germany) either received a single injection of monocrotaline (MCT, 60 mg/kg, s.c.) or saline. Three weeks after MCT injection, osmotic minipumps containing treprostinil (0.15 mg/mL; to deliver an approximate rate of 45 ng/kg/min) or saline vehicle were implanted for a further 2 weeks. Six animals were used per group.

RNA isolation, cDNA synthesis and reverse transcriptase PCR (RT-PCR)
Frozen lung tissue was homogenized and total RNA extracted with Trizol reagent (Invitrogen) according to the manufacturer's instructions. DNA was removed by TURBO DNA-free TURBO DNase treatment and removal reagents (Ambion). Reverse transcription was then performed with

the StrataScript first-strand synthesis system (Stratagene). Quantitative-PCR was performed using SYBR1 Green ER qPCR SuperMix, and samples were run on ABI step one machine.

Statistical Analysis
Analysis of data was carried out using the JMP software. The data was expressed as mean $\pm$ SD and analyzed using the student's T-test. One way analysis of variance (ANOVA) followed by Tukey's post hoc tests were carried out for comparision of multiple means. A P-value of ≤ 0.05 indicated statistical significance.

Results

Beraprost sodium (BPS) inhibits excessive cell proliferation in mutant mouse PASMCs
Abnormal proliferation is a characteristic feature of the vascular remodeling observed in PAH. Therefore, the impact of a prostacyclin analogue beraprost sodium (BPS) on cellular proliferation was investigated in mouse primary PASMCs harbouring a disease causing *BMPR2* nonsense mutation (*bmpr2* $^{R899X+/-}$). The mutant PASMCs proliferated more rapidly compared to wild-type (Figure 1A). Treatment with BPS inhibited proliferation in a dose-dependent manner and its anti-proliferative effects were higher in mutant PASMCs than in wild-type at the three highest doses used (Figure 1B). Next, we investigated whether BPS treatment increased cAMP production in these cells using the luminescence-based cAMP-Glo ^{TM} Assay kit (Promega). The luminescence generated in this assay is inversely proportional to the cAMP levels. BPS treatment inhibited luminescence activity in both wild-type and *bmpr2* $^{R899X+/-}$ PASMCs and this effect was higher in *bmpr2* $^{R899X+/-}$ cells compared with the wild-type (Figure 1C) suggesting that BPS-mediated cAMP production was higher in mutant cells.

We recently reported that the expression of plasminogen activator inhibitor (*PAI*-1), a recognized target of TGF-β signaling (23) was increased in mutant cells compared to the wild-type adding weight to the evidence for overactive TGF-β signaling in the mutant cells (24). Neither the expression of TGF-β1 ligand and nor the type II TGFBR2 receptor was altered in either cell type (Supplementary Figure 1 A-B) and BPS exhibited no discernible effect on the expression of these genes in both wild type and *bmpr2* $^{R899X+/-}$ PASMCs (Supp. Fig. 1C-D).

Beraprost restricts TGF-β–induced, pro-proliferative activity in *BMPR2*-deficient PASMCs
The effect of TGF-β1 ligand stimulation on the proliferation of *bmpr2*$^{+/+}$ and *bmpr2* $^{R899X+/-}$ PASMCs was examined. TGF-β1 was observed to have opposing effects on these cells, promoting proliferation in *bmpr2* $^{R899X+/-}$ cells in a dose-dependent manner, while showing no significant level of inhibition of proliferation in *bmpr2*$^{+/+}$ cells (Figure. 2A). The pro-proliferative effect of TGF-β1 in *bmpr2* $^{R899X+/-}$ cells is abrogated by the TGF-β signaling inhibitor (ALK5 inhibitor), SD208 (Figure 2B). In addition, the p38MAPK inhibitor, SB203580 significantly reduced TGF-β1 stimulated proliferation of *bmpr2* $^{R899X+/-}$ PASMCs (Figure 2C). Of note, both SD208 and SB203580 had previously been found to inhibit basal level of proliferation of mutant cells (24). Finally, BPS treatment also inhibited TGF-β1–stimulated proliferation of mutant PASMCs (Figure 2D).

BPS inhibits TGF-β-stimulated SMAD-responsive reporter activity
Next, the inhibition of TGF-β activity by *BMPR2* was investigated using a SMAD3 responsive SBE-Luc reporter assay in HEK293 cells (25). The overexpression of TGFBRII and TGF-β1 stimulation increased the reporter activity supporting the validity of this assay system (Supp 2A-B). The expression of wild-type BMPR-II reduced TGF-β–induced reporter activation, suggesting

a negative feedback loop between these two pathways (Figure 3A). Expression of BMPR-II with pathogenic mutations in the ligand binding (p.C118W) and kinase (p.C347Y and p.D485G) domains resulted in a failure to attenuate TGF-β activity. However, the expression of each mutant receptor showed differential effects on TGF-β-induced reporter activity compared with the wild-type. The anti-TGF-β effect of the p.D485G and p.C118W mutant receptors was significantly reduced compared with the wild type whilst p.C347Y mutant receptor showed no significant effect.

Next, the effect of BPS treatment on the TGF-β pathway was measured. BPS inhibited both basal (Figure 3B) and TGF-β1–stimulated (Figure 3C) SBE-Luc reporter activity in HEK293 cells in a dose-dependent manner. Furthermore, the expression of constitutively active TGF-β receptor type II (TGFBRII) increased reporter activity, and BPS inhibited this activation (Figure 3D). These findings suggest that BPS-mediated inhibition of TGF-β activity is mediated via a SMAD3/4-dependent pathway. BPS-mediated reporter inhibition of TGF-β signaling was reversed by a PKA inhibitor (KT5720) in the presence of TGFBRII overexpression (Figure 3E) and TGF-β1 ligand stimulation (Figure 3F) in a dose-dependent manner. Of note, the compound KT5720 has also been found to elicit non-specific effects on other protein kinases (26). Taken together, these data imply that the inhibitory effect of BPS on SMAD pathways may be PKA dependent.

Effect of prostacyclin analogues and other targeted PAH therapies on TGF-β signaling

Various prostacyclin analogues including BPS, treprostinil and iloprost exhibit differential therapeutic efficacy. We therefore investigated their individual effects on TGF-β signaling. All three prostacyclin analogues significantly inhibited both TGFBRII and TGF-β1-mediated SBE-Luc reporter activation (Figure 4A-B). As a representation of the targeted PAH therapies, the effect of PDE5 inhibitor sildenafil citrate on TGF-β signaling was investigated. This PDE5 inihibitor attenuated TGFBR2-mediated reporter activation at a high concentration (10μM) but failed to inhibit the reporter activity at the lower concentration and had no effect on TGF-β1-mediated reporter activation

Phosphorylation of SMAD3 is inhibited by BPS

To confirm that BPS inhibited SMAD-dependent TGF-β signaling, the phosphorylation of SMAD3 was examined by Western blot analysis. It was found that TGF-β1 stimulation increased the phosphorylation of SMAD3, and that BPS inhibited this phosphorylation in HEK293 cells (Figure 5A). TGF-β1–stimulated SMAD3 phosphorylation is also increased in *bmpr2* $^{R899X+/-}$ PASMCs compared to *bmpr2*$^{+/+}$ cells, and BPS treatment inhibited this TGF-β1 induced SMAD3 phosphorylation in both cell types (Figure 5B-C). Furthermore, phosphorylation of the linker region of SMAD2 was found to be reduced following BPS treatment (Figure 5D).

The pro-proliferative response of TGF-β1 is also mediated via the SMAD-independent p38MAPK pathway and inhibited by BPS treatment

Next, the effect of BPS on the TGF-β–mediated SMAD-independent pathway was investigated. In *bmpr2* $^{R899X+/-}$ PASMCs, the basal level of p38MAPK phosphorylation was increased compared to wild-type PASMCs (Figure 6A-B). Stimulation of the cells with TGF-β1 ligand further activated p38MAPK phosphorylation in *bmpr2* $^{R899X+/-}$ cells, and BPS treatment significantly inhibited TGF-β1–induced p38MAPK phosphorylation in a dose-dependent manner (Figures 6A-B). In HEK293 cells, the overexpression of TGFBRII increased phosphorylation of p38MAPK, and both BPS and TPS reduced this phosphorylation (Figure 6C). In these cells, both

BPS and TPS treatments elicited no discernible effects on the expression of total p38MAPK as well as SMAD2/3 proteins (Supp. Fig. 3)

Treprostinil (TPS) inhibits the TGF-β–induced SMAD pathway in monocrotaline-induced PAH rat lungs

The therapeutic potential of treprostinil (TPS), a stable prostacyclin analogue, was investigated in the MCT-induced PAH rat model which exhibited severe elevation of right ventricular systolic pressure, elevated pulmonary vascular resistance, and right ventricular hypertrophy and TPS treatment inhibited the progression of disease in these MCT-induced rats (27) .Western blot analysis of rat lungs following exposure to monocrotaline showed significantly increased SMAD3 phosphorylation, which was inhibited upon TPS treatment (Figure 7A-B). In these extracts, TPS treatment exerted no discernible effects on the expression of total SMAD3 protein (Supp. Fig. 4A-B). An elevated level of *PAI-1* transcripts was observed in PAH rat lungs which was reduced following TPS treatment (Figure 7C).

Discussion

In this study, we provide insight into the mechanisms by which prostacyclin analogues inhibit BMPR-II-mediated proliferation defects that lead to the eventual vascular remodeling observed in PAH. We further demonstrate that *BMPR2* mutation potentiates TGF-β–mediated SMAD-dependent and -independent pathways. Prostanoids inhibit TGF-β signaling by inhibiting SMAD3 and SMAD-independent p38MAPK pathways. To the best of our knowledge, this is the first report demonstrating a potential mechanism by which prostacyclin analogues inhibit overactive TGF-β responses in PAH.

Elevated expression levels of TGF-β ligands have been reported in the serum of PAH patients (28) and in experimental models of PAH (29), (30), suggesting a link between the TGF-β pathway and PAH. We have demonstrated that the expression of BMPRII receptor attenuated TGF-β activity and this anti- TGF-β effect is diminished in cells expressing mutant receptors deficient in kinase activity (p. D485G) or cell-surface localization (p.C118W) (10), suggesting that defects in *BMPR*2 receptor may potentiate TGF-β signaling. It has not escaped our attention that the p.D485G mutant receptor but not the p.C347Y mutant activated the SBE-Luc reporter activity. The p.D485G mutant receptor showed no receptor activity (21) whilst the p.C347Y mutant elicited a reduced level of SMAD1/5 activity (31) implying that there may be a correlation between the level of *BMPR*2 receptor deficiency and the activation of TGF-β signaling. We have shown in a number of ways that the activation of the TGF-β pathway contributes to abnormal proliferation via SMAD-independent p38MAPK in PASMCs deficient in BMPR-II receptor. First, we have demonstrated that TGF-β1 stimulation promotes proliferation in *bmpr2* $^{R899X+/-}$ PASMCs in a dose-dependent manner. Second, we show that in the wild-type PASMCs, this ligand does not increase proliferation but significantly enhances phosphorylation of SMAD3 protein indicating that the TGF-β-induced pro-proliferative activity in mutant cells is mediated via SMAD-independent pathways (24, 32). Third, we have shown that selective inhibition of p38MAPK using the small molecule inhibitor SB203580 inhibits the pro-proliferative response to TGF-β1 ligand in these mutant cells in a dose-dependent manner.

Emerging evidence supports the role of p38MAPK in the pathogenesis of pulmonary vascular remodeling, a process that has been shown to be regulated by BMPs and TGF-βs, cellular stress and inflammatory cytokines (33). Hypoxia induces p38MAPK phosphorylation in pulmonary arteries and induces proliferation of human PASMCs (34). Inhibition of this pathway reverses hypoxia-induced pulmonary arterial dysfunction, including endothelium-dependent relaxation (5),

(9). Transfection of mutant, but not wild-type, *BMPR2* constructs activates p38MAPK phosphorylation in a mouse epithelial cell line (NMuMG), generating a pro-proliferative response (10). PAH-PASMCs harbouring a number of *BMPR2* mutations showed enhanced p38MAPK phosphorylation in response to BMP4 stimulation (35), supporting the involvement of this pathway in PAH. However, targeting the TGF-β/p38MAPK axis carries substantial risk due to its role in maintaining normal homeostasis. Therefore, the inhibition of this pathway requires a deeper understanding of TGF-β signaling and the context in which it acts, as well as the cellular consequences of its inhibition.

As prostacyclin therapy remains the first line treatment for patients with severe PAH, the mode of action of these drugs in mouse and human PASMCs and in the monocrotaline-induced PAH rat model was investigated. Several lines of evidence are provided that suggest that prostacyclin analogues are capable of inhibiting TGF-β–induced SMAD-dependent and -independent pathways in mouse primary PASMCs and PAH-PASMCs. First, it was demonstrated that beraprost sodium inhibits abnormal cell proliferation in mouse PASMCs in a dose-dependent manner in both the absence and presence of TGF-β stimulation. Second, it was shown that the drug is capable of inhibiting TGF-β1–induced SMAD-independent p38MAPK phosphorylation in mouse PASMCs and TGFBRII-induced p38MAPK phosphorylation in HEK293 cells. Third, evidence was provided that this chemical inhibits the TGFβ-SMAD axis by inhibiting the phosphorylation of SMAD 3 protein in these cells. Finally, *in vivo* support of the *in vitro* findings was provided in the monocrotaline-induced PAH rat model, in which the expression of BMPR-II receptor is reduced and the TGFβ pathway is activated (14), (24). In the MCT-induced rat model, treprostinil infusion attenuated over-active TGF-β1 signaling by inhibiting the phosphorylation of SMAD3. It remains unknown as to how prostacyclin analogues elicit anti-TGF-β activity. Our data suggest that this anti-TGF-β effect may be mediated through the PKA-dependent pathway and the drug may modulate the activity of the TGFBRII receptor. However, further studies are required to understand the molecular mechanisms by which prostacyclin analogues interfere with TGF-β signaling.

Although prostacyclin-mediated vasodilator and anticoagulant activities are well described, the mechanisms by which these drugs exert their anti-proliferative effects are not well understood. Prostanoids have been shown to inhibit proliferation in PAH-PASMCs and this effect appears to be mediated via a PKA-dependent pathway (18), which is consistent with our observations. Our data suggest that the anti-proliferative effects of BPS may be mediated through the cAMP-PKA-dependent pathway as the mutant cells produced an elevated level of cAMP and showed an enhanced anti-proliferative effect compared with control PASMCs in response to BPS. Together, these observations indicate that *BMPR*2 mutation may impair the prostacyclin- cAMP-PKA pathway which may contribute to the activation of TGF-β signaling, and prostacyclin analogues exert anti- TGF-β effects through the elevation of cAMP-PKA pathway. Increased plasma cAMP levels were observed in healthy subjects following prostacyclin inhalation (36) but the association between elevated cAMP levels and clinical outcome of PAH has not been established. As G-protein coupled receptor (GPCR)-mediated signaling and phosphodiesterase inhibitors raise the level of cAMP (37), it would be interesting to investigate whether they elicit anti-TGF-β effects in PAH. Of note, the anti-proliferative effect of prostanoids has also been reported to be regulated through PKA-independent PPARγ and -β pathways (38), (39). In PAH, the imbalance between TGF-β and BMP signaling events contributes to the initial stages of vascular remodeling (40) and thus a balance between these two pathways may provide a target for therapeutic intervention. We demonstrated previously that prostacyclins restore the balance in part through the elevation of BMP signaling in PAH-PASMCs and in the monocrotaline-induced rat model which are

associated with reduced BMPR-II expression (27). Here, we show that these drugs also inhibit overactive TGF-β signaling in mouse PASMCs harbouring a nonsense mutation in the *BMPR2* gene. Taken together, these data indicate that the benefits of these drugs may be stronger in patients with loss of function BMPR-II mutations.

In conclusion, we have demonstrated that dysfunctional BMPR-II-mediated signaling leads to increased TGF-β signaling, inducing both SMAD-dependent and -independent p38MAPK pathways, and that prostanoids play an essential role in fine tuning the effects of BMP and TGF-β in the treatment of PAH. Given the preventative potential of these drugs in animal models (27), we propose that the inhibition of increased TGF-β activity via prostacyclins may be an effective prophylactic intervention in PAH.

Acknowledgements
The authors express sincere thanks to Ms Bethan Jones for critically reading through the manuscript and Ms Seshu Kanneganti for technical assistance. This work was supported by a fellowship (awarded to MTN) from the Department of Health via the NIHR Comprehensive Biomedical Research Centre award to Guy's & St Thomas' NHS Foundation Trust in partnership with King's College London and the Cambridge NIHR Biomedical Research Centre. The authors acknowledge financial support from the British Heart foundation, UK (programme grant 1-2004-357 to RCT), and to NWM, Heptagon Life Science Proof of Concept Fund (grants KCL24 and KCL25 to MTN and RCT, respectively) and the Great Britain Sasakawa Foundation (B70 to MTN).

Disclosures
None.

References
1. Lane KB, Machado RD, Pauciulo MW, Thomson JR, Phillips JA, 3rd, Loyd JE, Nichols WC, Trembath RC. Heterozygous germline mutations in bmpr2, encoding a tgf-beta receptor, cause familial primary pulmonary hypertension. The international pph consortium. *Nat Genet* 2000;26:81-84.
2. Machado RD, Aldred MA, James V, Harrison RE, Patel B, Schwalbe EC, Gruenig E, Janssen B, Koehler R, Seeger W, et al. Mutations of the tgf-beta type ii receptor bmpr2 in pulmonary arterial hypertension. *Hum Mutat* 2006;27:121-132.
3. Runo JR, Loyd JE. Primary pulmonary hypertension. *Lancet* 2003;361:1533-1544.
4. Yang X, Long L, Southwood M, Rudarakanchana N, Upton PD, Jeffery TK, Atkinson C, Chen H, Trembath RC, Morrell NW. Dysfunctional smad signaling contributes to abnormal smooth muscle cell proliferation in familial pulmonary arterial hypertension. *Circ Res* 2005;96:1053-1063.
5. Welsh DJ, Peacock AJ, MacLean M, Harnett M. Chronic hypoxia induces constitutive p38 mitogen-activated protein kinase activity that correlates with enhanced cellular proliferation in fibroblasts from rat pulmonary but not systemic arteries. *Am J Respir Crit Care Med* 2001;164:282-289.
6. Zeng Z, Li Y, Jiang Z, Wang C, Li B, Jiang W. The extracellular signal-regulated kinase is involved in the effects of sildenafil on pulmonary vascular remodeling. *Cardiovasc Ther*;28:23-29.
7. Long L, MacLean MR, Jeffery TK, Morecroft I, Yang X, Rudarakanchana N, Southwood M, James V, Trembath RC, Morrell NW. Serotonin increases susceptibility to pulmonary hypertension in bmpr2-deficient mice. *Circ Res* 2006;98:818-827.

8. West J, Harral J, Lane K, Deng Y, Ickes B, Crona D, Albu S, Stewart D, Fagan K. Mice expressing bmpr2r899x transgene in smooth muscle develop pulmonary vascular lesions. *Am J Physiol Lung Cell Mol Physiol* 2008;295:L744-755.
9. Weerackody RP, Welsh DJ, Wadsworth RM, Peacock AJ. Inhibition of p38 mapk reverses hypoxia-induced pulmonary artery endothelial dysfunction. *Am J Physiol Heart Circ Physiol* 2009;296:H1312-1320.
10. Rudarakanchana N, Flanagan JA, Chen H, Upton PD, Machado R, Patel D, Trembath RC, Morrell NW. Functional analysis of bone morphogenetic protein type ii receptor mutations underlying primary pulmonary hypertension. *Hum Mol Genet* 2002;11:1517-1525.
11. Nishihara A, Watabe T, Imamura T, Miyazono K. Functional heterogeneity of bone morphogenetic protein receptor-ii mutants found in patients with primary pulmonary hypertension. *Mol Biol Cell* 2002;13:3055-3063.
12. Atkinson C, Stewart S, Imamura T, Trembath RC, Morrell NW. Immunolocalisation of bmpr-ii and tgf-ss type i and ii receptors in primary plexogenic pulmonary hypertension. *J Heart Lung Transplant* 2001;20:149.
13. Mata-Greenwood E, Meyrick B, Steinhorn RH, Fineman JR, Black SM. Alterations in tgf-beta1 expression in lambs with increased pulmonary blood flow and pulmonary hypertension. *Am J Physiol Lung Cell Mol Physiol* 2003;285:L209-221.
14. Long L, Crosby A, Yang X, Southwood M, Upton PD, Kim DK, Morrell NW. Altered bone morphogenetic protein and transforming growth factor-beta signaling in rat models of pulmonary hypertension: Potential for activin receptor-like kinase-5 inhibition in prevention and progression of disease. *Circulation* 2009;119:566-576.
15. Richter A, Yeager ME, Zaiman A, Cool CD, Voelkel NF, Tuder RM. Impaired transforming growth factor-beta signaling in idiopathic pulmonary arterial hypertension. *Am J Respir Crit Care Med* 2004;170:1340-1348.
16. Morrell NW, Yang X, Upton PD, Jourdan KB, Morgan N, Sheares KK, Trembath RC. Altered growth responses of pulmonary artery smooth muscle cells from patients with primary pulmonary hypertension to transforming growth factor-beta(1) and bone morphogenetic proteins. *Circulation* 2001;104:790-795.
17. Tawara S, Fukumoto Y, Shimokawa H. Effects of combined therapy with a rho-kinase inhibitor and prostacyclin on monocrotaline-induced pulmonary hypertension in rats. *J Cardiovasc Pharmacol* 2007;50:195-200.
18. Wharton J, Davie N, Upton PD, Yacoub MH, Polak JM, Morrell NW. Prostacyclin analogues differentially inhibit growth of distal and proximal human pulmonary artery smooth muscle cells. *Circulation* 2000;102:3130-3136.
19. Stratton R, Shiwen X, Martini G, Holmes A, Leask A, Haberberger T, Martin GR, Black CM, Abraham D. Iloprost suppresses connective tissue growth factor production in fibroblasts and in the skin of scleroderma patients. *J Clin Invest* 2001;108:241-250.
20. Stratton R, Rajkumar V, Ponticos M, Nichols B, Shiwen X, Black CM, Abraham DJ, Leask A. Prostacyclin derivatives prevent the fibrotic response to tgf-beta by inhibiting the ras/mek/erk pathway. *FASEB J* 2002;16:1949-1951.
21. Nasim MT, Ghouri A, Patel B, James V, Rudarakanchana N, Morrell NW, Trembath RC. Stoichiometric imbalance in the receptor complex contributes to dysfunctional bmpr-ii mediated signalling in pulmonary arterial hypertension. *Hum Mol Genet* 2008;17:1683-1694.
22. Nasim MT, Eperon IC. A double-reporter splicing assay for determining splicing efficiency in mammalian cells. *Nature Protocols* 2006;1:1022-1028.
23. Thomas M, Docx C, Holmes AM, Beach S, Duggan N, England K, Leblanc C, Lebret C, Schindler F, Raza F, et al. Activin-like kinase 5 (alk5) mediates abnormal proliferation of vascular smooth muscle cells from patients with familial pulmonary arterial hypertension and is

involved in the progression of experimental pulmonary arterial hypertension induced by monocrotaline. *Am J Pathol* 2009;174:380-389.
24. Nasim MT, Ogo T, Chowdhury HM, Zhao L, Chen CN, Rhodes C, Trembath RC. Bmpr-ii deficiency elicits pro-proliferative and anti-apoptotic responses through the activation of tgfbeta-tak1-mapk pathways in pah. *Hum Mol Genet*;21:2548-2558.
25. Dennler S, Itoh S, Vivien D, ten Dijke P, Huet S, Gauthier JM. Direct binding of smad3 and smad4 to critical tgf beta-inducible elements in the promoter of human plasminogen activator inhibitor-type 1 gene. *Embo J* 1998;17:3091-3100.
26. Murray AJ. Pharmacological pka inhibition: All may not be what it seems. *Sci Signal* 2008;1:re4.
27. Yang J, Li X, Al-Lamki RS, Southwood M, Zhao J, Lever AM, Grimminger F, Schermuly RT, Morrell NW. Smad-dependent and smad-independent induction of id1 by prostacyclin analogues inhibits proliferation of pulmonary artery smooth muscle cells in vitro and in vivo. *Circ Res*;107:252-262.
28. Selimovic N, Bergh CH, Andersson B, Sakiniene E, Carlsten H, Rundqvist B. Growth factors and interleukin-6 across the lung circulation in pulmonary hypertension. *Eur Respir J* 2009;34:662-668.
29. Arcot SS, Lipke DW, Gillespie MN, Olson JW. Alterations of growth factor transcripts in rat lungs during development of monocrotaline-induced pulmonary hypertension. *Biochem Pharmacol* 1993;46:1086-1091.
30. Jiang Y, Dai A, Li Q, Hu R. Hypoxia induces transforming growth factor-beta1 gene expression in the pulmonary artery of rats via hypoxia-inducible factor-1alpha. *Acta Biochim Biophys Sin (Shanghai)* 2007;39:73-80.
31. Yang J, Davies RJ, Southwood M, Long L, Yang X, Sobolewski A, Upton PD, Trembath RC, Morrell NW. Mutations in bone morphogenetic protein type ii receptor cause dysregulation of id gene expression in pulmonary artery smooth muscle cells: Implications for familial pulmonary arterial hypertension. *Circ Res* 2008;102:1212-1221.
32. Davies RJ, Holmes AM, Deighton J, Long L, Yang X, Barker L, Walker C, Budd DC, Upton PD, Morrell NW. Bmp type ii receptor deficiency confers resistance to growth inhibition by tgf-beta in pulmonary artery smooth muscle cells: Role of proinflammatory cytokines. *Am J Physiol Lung Cell Mol Physiol*;302:L604-615.
33. Massague J. Integration of smad and mapk pathways: A link and a linker revisited. *Genes Dev* 2003;17:2993-2997.
34. Chen B, Calvert AE, Cui H, Nelin LD. Hypoxia promotes human pulmonary artery smooth muscle cell proliferation through induction of arginase. *Am J Physiol Lung Cell Mol Physiol* 2009;297:L1151-1159.
35. Dewachter L, Adnot S, Guignabert C, Tu L, Marcos E, Fadel E, Humbert M, Dartevelle P, Simonneau G, Naeije R, et al. Bone morphogenetic protein signalling in heritable versus idiopathic pulmonary hypertension. *Eur Respir J* 2009;34:1100-1110.
36. Beghetti M, Reber G, de MP, Vadas L, Chiappe A, Spahr-Schopfer I, Rimensberger PC. Aerosolized iloprost induces a mild but sustained inhibition of platelet aggregation. *Eur Respir J* 2002;19:518-524.
37. Pullamsetti SS, Savai R, Schaefer MB, Wilhelm J, Ghofrani HA, Weissmann N, Schudt C, Fleming I, Mayer K, Leiper J, et al. Camp phosphodiesterase inhibitors increases nitric oxide production by modulating dimethylarginine dimethylaminohydrolases. *Circulation* 2011;123:1194-1204.
38. Falcetti E, Hall SM, Phillips PG, Patel J, Morrell NW, Haworth SG, Clapp LH. Smooth muscle proliferation and role of the prostacyclin (ip) receptor in idiopathic pulmonary arterial hypertension. *Am J Respir Crit Care Med*;182:1161-1170.

39. Ali FY, Egan K, FitzGerald GA, Desvergne B, Wahli W, Bishop-Bailey D, Warner TD, Mitchell JA. Role of prostacyclin versus peroxisome proliferator-activated receptor beta receptors in prostacyclin sensing by lung fibroblasts. *Am J Respir Cell Mol Biol* 2006;34:242-246.
40. ten Dijke P, Arthur HM. Extracellular control of tgfbeta signalling in vascular development and disease. *Nat Rev Mol Cell Biol* 2007;8:857-869.

Figure legends

Figure 1
Inhibition of abnormal cell proliferation by beraprost sodium (BPS) and effect on cAMP production. Twenty four hours after seeding wild-type (WT *bmpr2* $^{+/+)}$ and mutant (*bmpr2* $^{R899X+/-}$) mouse primary PASMCs, the medium was replaced with DMEM/0.1%FCS with or without BPS and following incubation for 3-4 days proliferation was measured using the CellTiter 96® Aq_{ueous} One Solution Cell Proliferation Assay (Promega) (A,B), in the presence of increasing concentrations of BPS (B) or cAMP production measured using the cAMP Glo Assay kit (Promega) in the presence or absence of 10μM BPS (C). The luminescence generated in the cAMP Glo assay is inversely proportional to the cAMP levels. White bars/diamonds represent wild-type cells and filled black bars/squares represent mutant PASMCs. Results shown as a percentage of wild-type (A), or as a percentage of untreated cells (B, C). * - $p < 0.05$, ** - $p < 0.01$, *** - $p < 0.001$. Data are presented as the mean ± SD from at least 3 independent experiments.

Figure 2
The pro-proliferative response of TGF-β1 is inhibited by BPS. Proliferation was measured as in Fig 1 after mouse wild type (white bars) and/or mutant (black bars) PASMCs were incubated in DMEM/0.1% FCS for 3-4 days in the presence and absence of (A) increasing concentrations of TGFβ1, (B) ALK5 inhibitor, SD208 (10μM), (C) increasing concentrations of p38 MAPK inhibitor, SB203580 in the presence of 10ng/ml TGF-β1 and (D) increasing concentrations of BPS in the presence of 10ng/ml TGF-β1. All results expressed as a percentage of untreated cells. NS – non significant, * - $p < 0.05$, ** - $p < 0.01$, *** - $p < 0.001$. Data are presented as the mean ± SD from 3-6 independent experiments.

Figure 3
Inhibition of SMAD responsive reporter activity by beraprost. Transient transfections of reporter plasmids with or without additional plasmids containing either the wild-type or mutated BMPR2 or TGFBRII in HEK293 cells. Twenty four hours after transfection, the medium was replaced by DMEM/0.1% FCS in the presence or absence of TGF-β1 and/or BPS or KT5720 and incubated for a further 16 hours. Luciferase and β-Galactosidase activities were measured using the Tropix Dual Light Assay (Applied Biosystems). The luc/gal ratio of untreated cells with no additional plasmids was set as 100. (A) Cells transfected with reporter plasmids only (control) or reporter plasmids together with a plasmid encoding either wild-type BMPR2 or mutated BMPR2 (pC118W, pC347Y and pD485G) in the presence or absence of 10ng/ml of TGF-β1. Transfection of reporter plasmids in the presence of increasing concentrations of BPS in the absence (B) and presence of 10ng/ml TGF-β1 stimulation (C). (D) Cells transfected with reporter plasmids and a plasmid containing the wild-type TGFBRII or stimulated with 10ng/ml TGF-β1in the presence or absence of 10μM BPS. As in (D), in the presence of increasing concentrations PKA inhibitor KT5720 in cells overexpressed with TGFBRII receptor (E) and stimulated with TGFβ1 (F). NS –

non significant, * - $p < 0.05$, ** - $p < 0.01$, *** - $p < 0.001$, compared to untreated controls unless otherwise indicated. Data are presented as the mean ± SD from 3-6 independent experiments.

Figure 4

Inhibition TGF-β signaling by prostacyclin analogues and PDE5 inhibitor, sildenafil citrate. As in Fig 3(D), following treatment with prostacyclin analogues Beraprost Sodium (BPS), Treprostinil (TPS) and Iloprost (ILO) and the PDE5 inhibitor Sildenafil citrate (PDE5) at concentrations of 10μM and 1μM as well as SD208 (10μM) in the presence of TGFBRII overexpression (A) and (B) TGF-β1 stimulation. The recognised ALK5 inhibitor SD208 was used as a positive control. The Luc/Gal ratio of untreated cells was set as 100. NS – non significant, * - $p < 0.05$, ** - $p < 0.01$, *** - $p < 0.001$, in comparison with untreated cells. Data are presented as the mean ± SD from 3 independent experiments.

Figure 5

BPS inhibits SMAD3 phosphorylation (Ser423/425) in HEK293 and mouse primary PASMCs. (A) Phospho-SMAD3 levels in HEK293 cells were detected by western blot with and without one hour of TGF-β1stimulation in the presence of increasing concentrations of BPS. (B) Phospho-SMAD3 levels in wild-type (WT *bmpr2* $^{+/+}$) and mutant (*bmpr2* $^{R899X+/-}$) mouse primary PASMCs were detected by western blot in the presence and absence of 10ng/ml TGF-β1 and 1, 5 and 10μM BPS. (C) Quantification of phospho-SMAD3 levels relative to β-actin from wild-type (white bars) and mutant (black bars) PASMCs derived from three independent experiments. * - $p < 0.05$, ** - $p < 0.01$ compared with TGF-β1stimulated cells. Western blot of phosphorylated SMAD2 (Ser245/250/255) in the presence and absence of TGF-β1(10ng/ml) and 10μM BPS in mutant PASMCs.

Figure 6

Inhibition of SMAD-independent p38MAPK pathways by BPS treatment. (A) Phosphorolated-p38MAPK levels in wild-type (WT *bmpr2* $^{+/+}$) and mutant (*bmpr2* $^{R899X+/-}$) mouse primary PASMCs were detected by western blot in the presence and absence of 10ng/ml TGF-β1 and 1, 5 and 10μM BPS. (B) Quantification of phosphorylated-p38MAPK levels relative to β-actin from wild-type (white bars) and mutant (black bars) PASMCs derived from three independent experiments. (C) Phosphorolated-p38MAPK levels in HEK293 cells were detected by western blot following TGFBRII overexpression in the presence and absence of BPS and TPS treatment. * - $p < 0.05$, ** - $p < 0.01$ compared with untreated or TGF-β1stimulated cells.

Figure 7

Inhibition of TGF-β signaling in monocrotaline (MCT)-induced PAH rat lungs by treprostinil (TPS) treatment. (A) Phospho-SMAD3 levels were detected by western blot in rat lungs following two weeks of treatment with MCT or MCT and TPS. (B) Quantification of phospho-SMAD3 levels relative to β-actin. (C) Relative expression of PAI-1 to β-actin transcripts in rat lungs following two weeks of treatment with MCT or MCT and TPS. * - $p < 0.05$, ** - $p < 0.01$ compared with control.

Figure 1

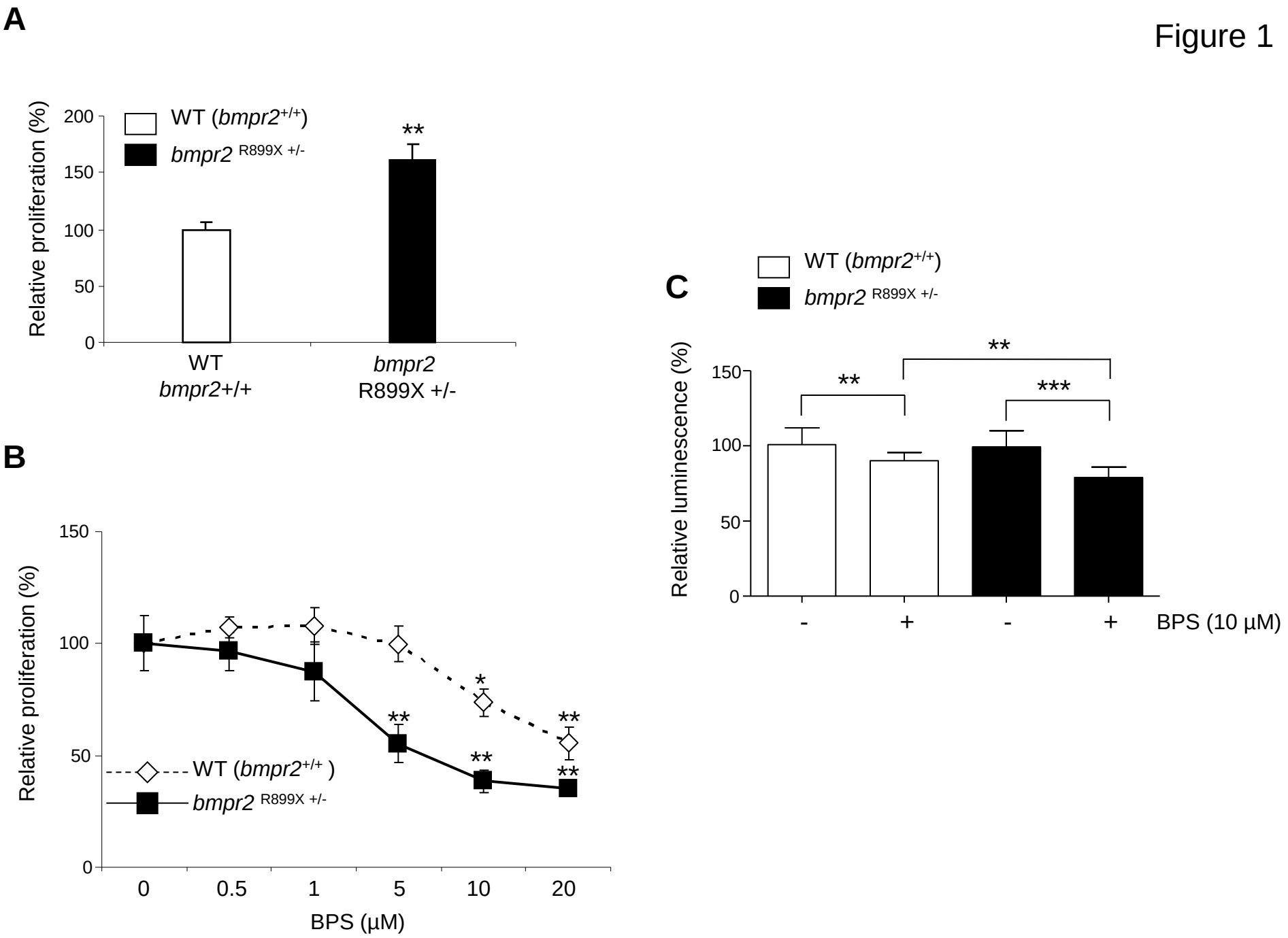
A
Relative proliferation (%)
200
150
100
50
0
WT (bmpr2+/+)
bmpr2 R899X +/-
**
WT
bmpr2+/+
bmpr2
R899X +/-
B
Relative proliferation (%)
150
100
50
0
WT (bmpr2+/+)
bmpr2 R899X +/-
*
**
**
**
**
0
0.5
1
5
10
20
BPS (μM)
C
WT (bmpr2+/+)
bmpr2 R899X +/-
Relative luminescence (%)
150
100
50
0
**
**
***
-
+
-
+
BPS (10 μM)

Figure 2

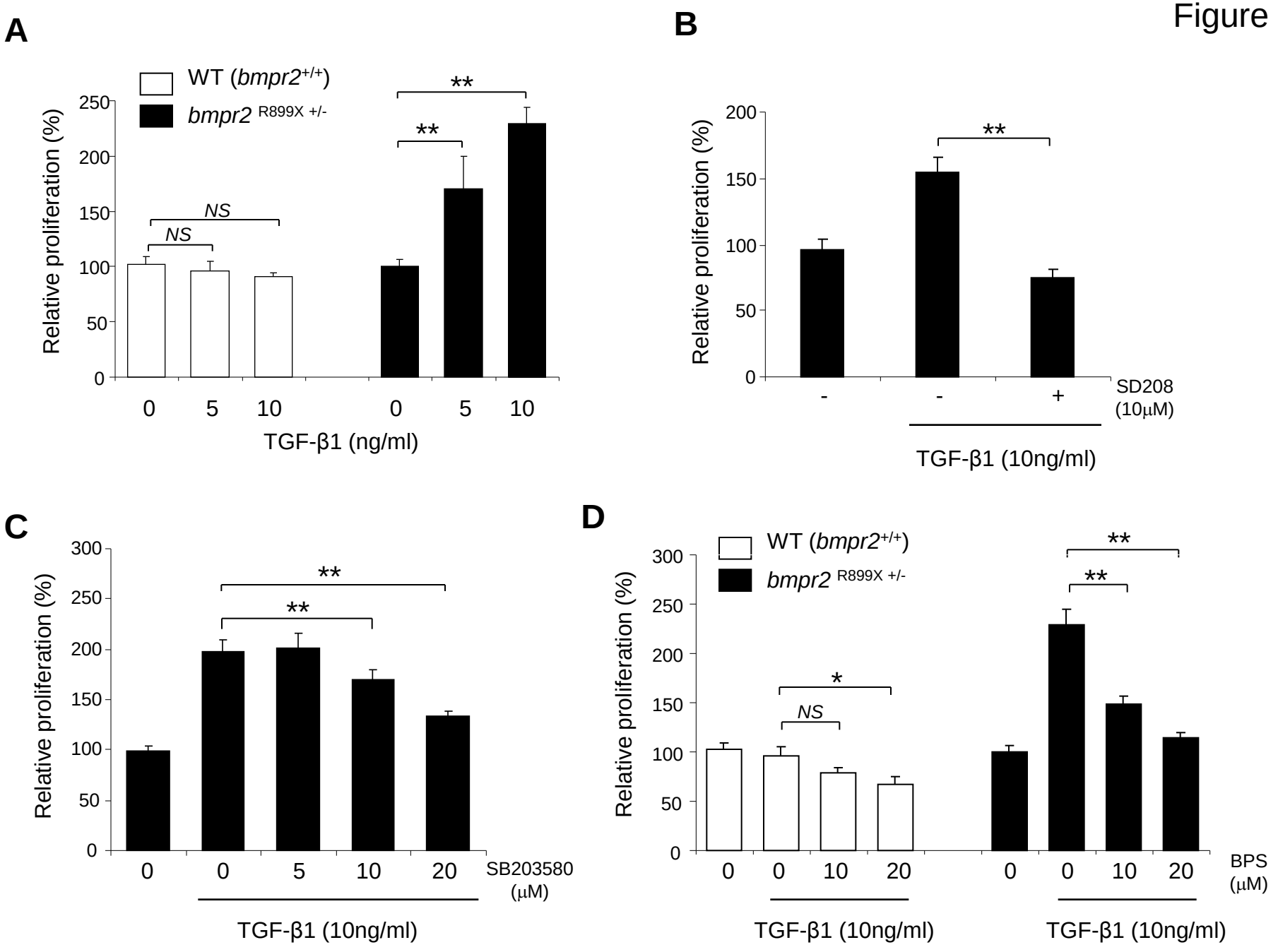
A
WT (bmpr2+/+)
bmpr2 R899X +/-
Relative proliferation (%)
250
200
150
100
50
0
NS
NS
**
**
0
5
10
0
5
10
TGF-β1 (ng/ml)
B
Relative proliferation (%)
200
150
100
50
0
**
-
-
+
SD208
(10μM)
TGF-β1 (10ng/ml)
C
Relative proliferation (%)
300
250
200
150
100
50
0
**
**
0
0
5
10
20
SB203580
(μM)
TGF-β1 (10ng/ml)
D
WT (bmpr2+/+)
bmpr2 R899X +/-
Relative proliferation (%)
300
250
200
150
100
50
0
*
NS
**
**
0
0
10
20
0
0
10
20
BPS
(μM)
TGF-β1 (10ng/ml)
TGF-β1 (10ng/ml)

Figure 3

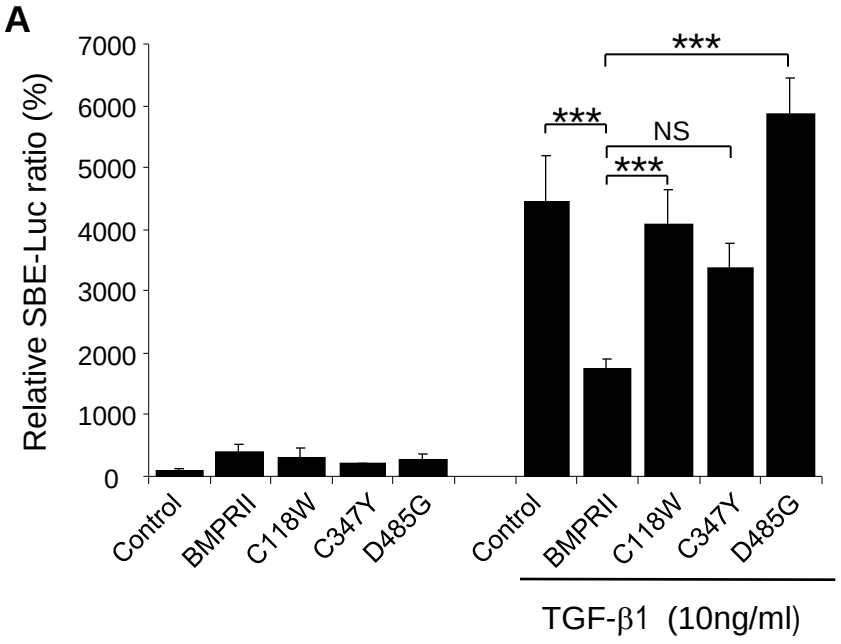
A
Relative SBE-Luc ratio (%)
7000
6000
5000
4000
3000
2000
1000
0
***
***
NS
***
Control
BMPRII
C118W
C347Y
D485G
Control
BMPRII
C118W
C347Y
D485G
TGF-β1 (10ng/ml)

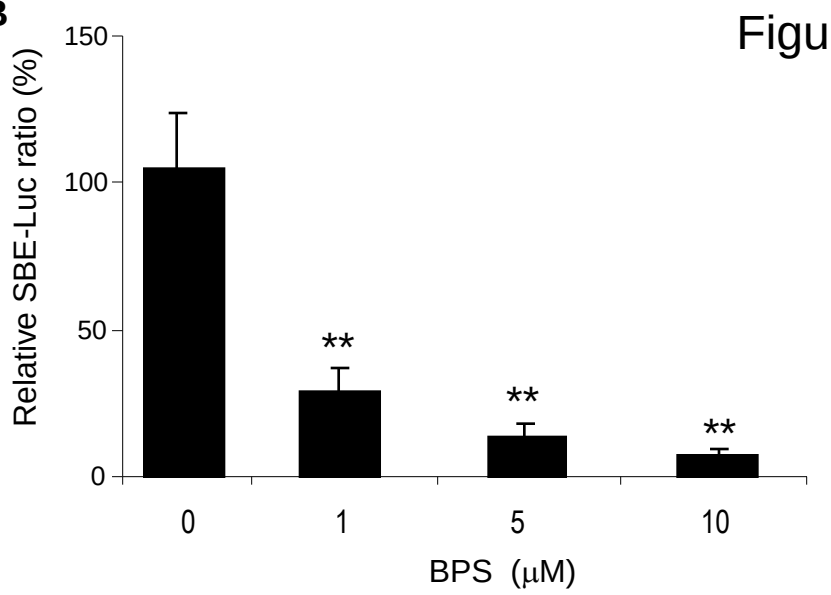
B
Relative SBE-Luc ratio (%)
150
100
50
0
**
**
**
0
1
5
10
BPS (μM)

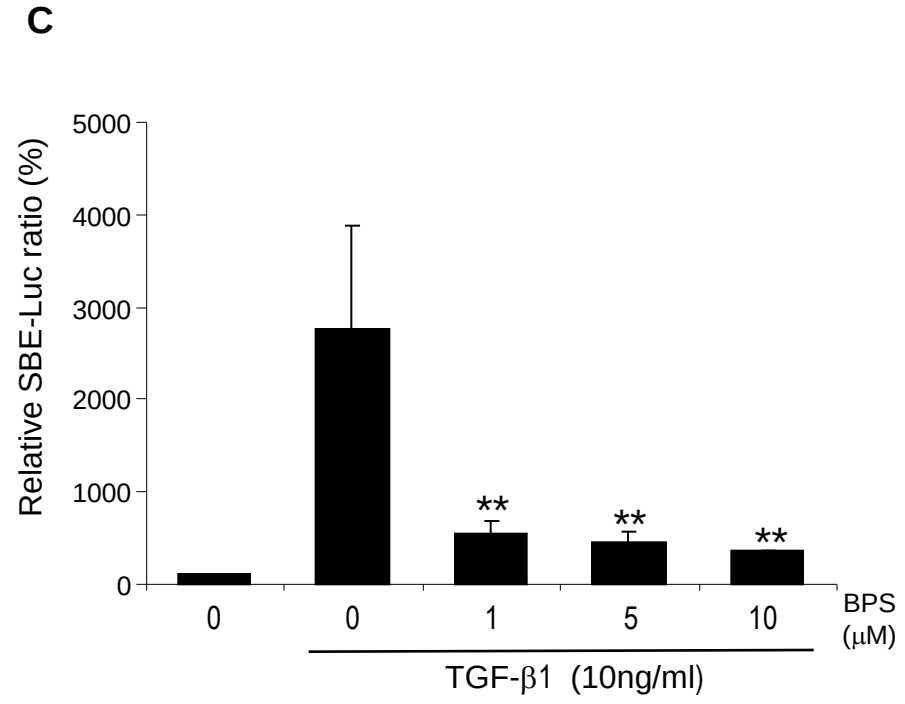
C
Relative SBE-Luc ratio (%)
5000
4000
3000
2000
1000
0
**
**
**
0
0
1
5
10
BPS (μM)
TGF-β1 (10ng/ml)

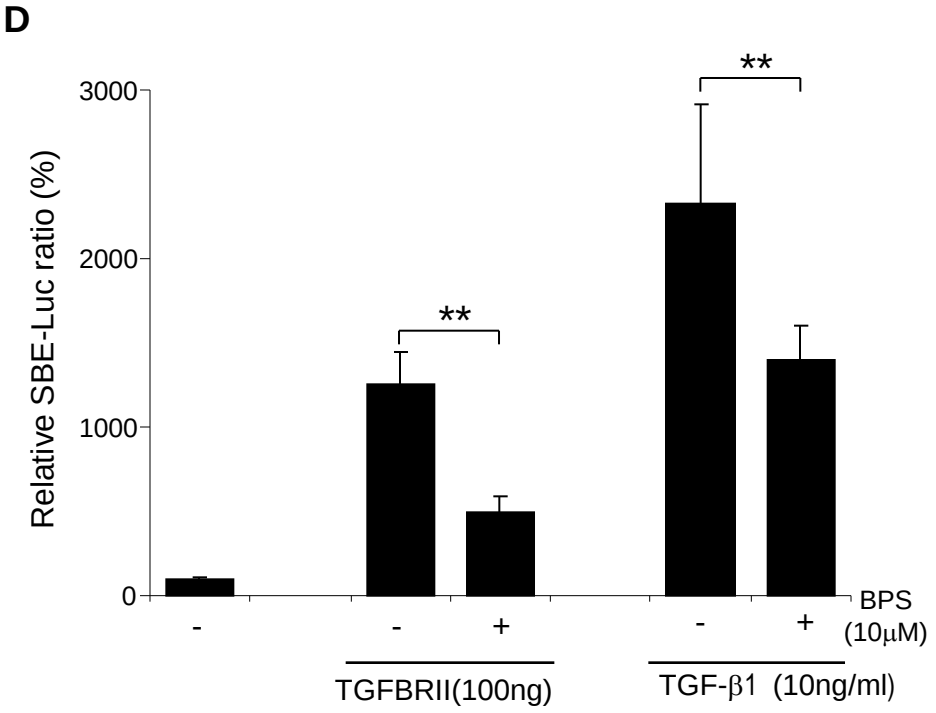
D
Relative SBE-Luc ratio (%)
3000
2000
1000
0
**
**
-
-
+
-
+
BPS (10μM)
TGFBRII(100ng)
TGF-β1 (10ng/ml)

Figure 3

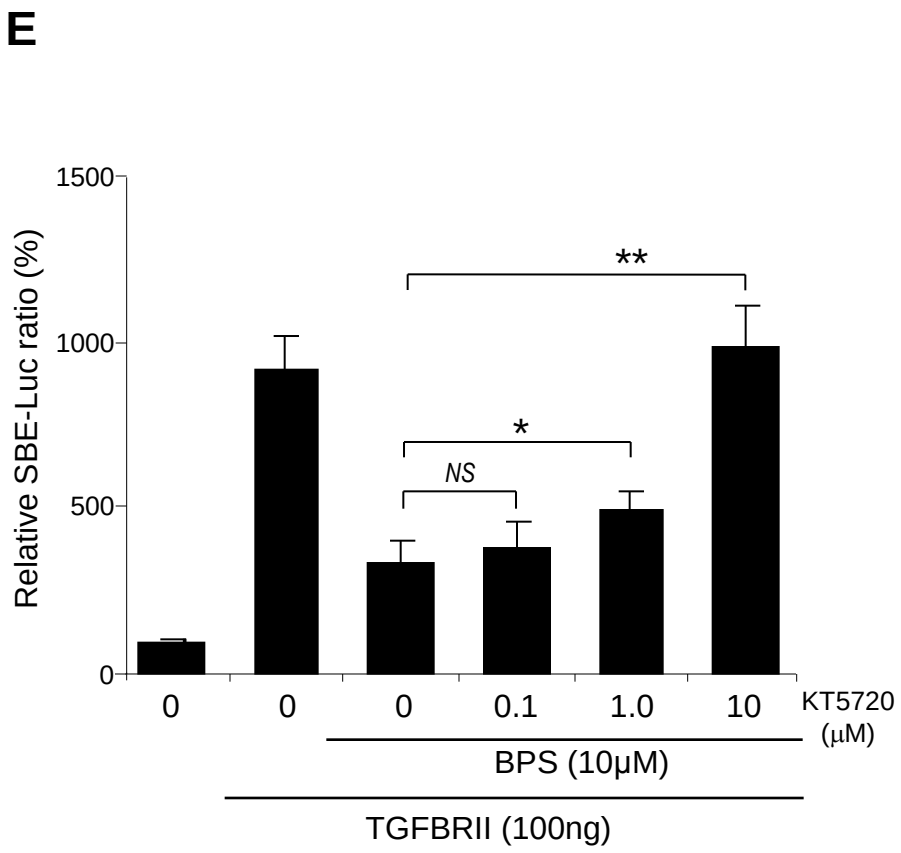
E
Relative SBE-Luc ratio (%)
1500
1000
500
0
**
*
NS
0
0
0
0.1
1.0
10
KT5720 (μM)
BPS (10μM)
TGFBRII (100ng)

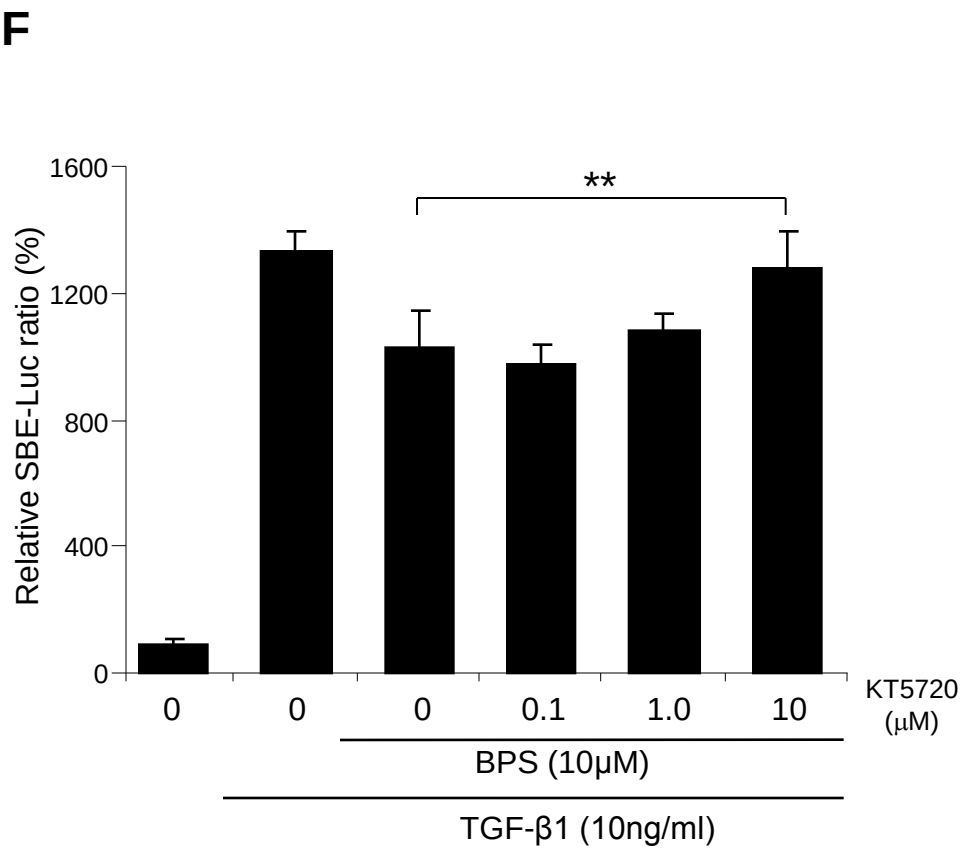
F
Relative SBE-Luc ratio (%)
1600
1200
800
400
0
**
0
0
0
0.1
1.0
10
KT5720 (μM)
BPS (10μM)
TGF-β1 (10ng/ml)

Figure 4

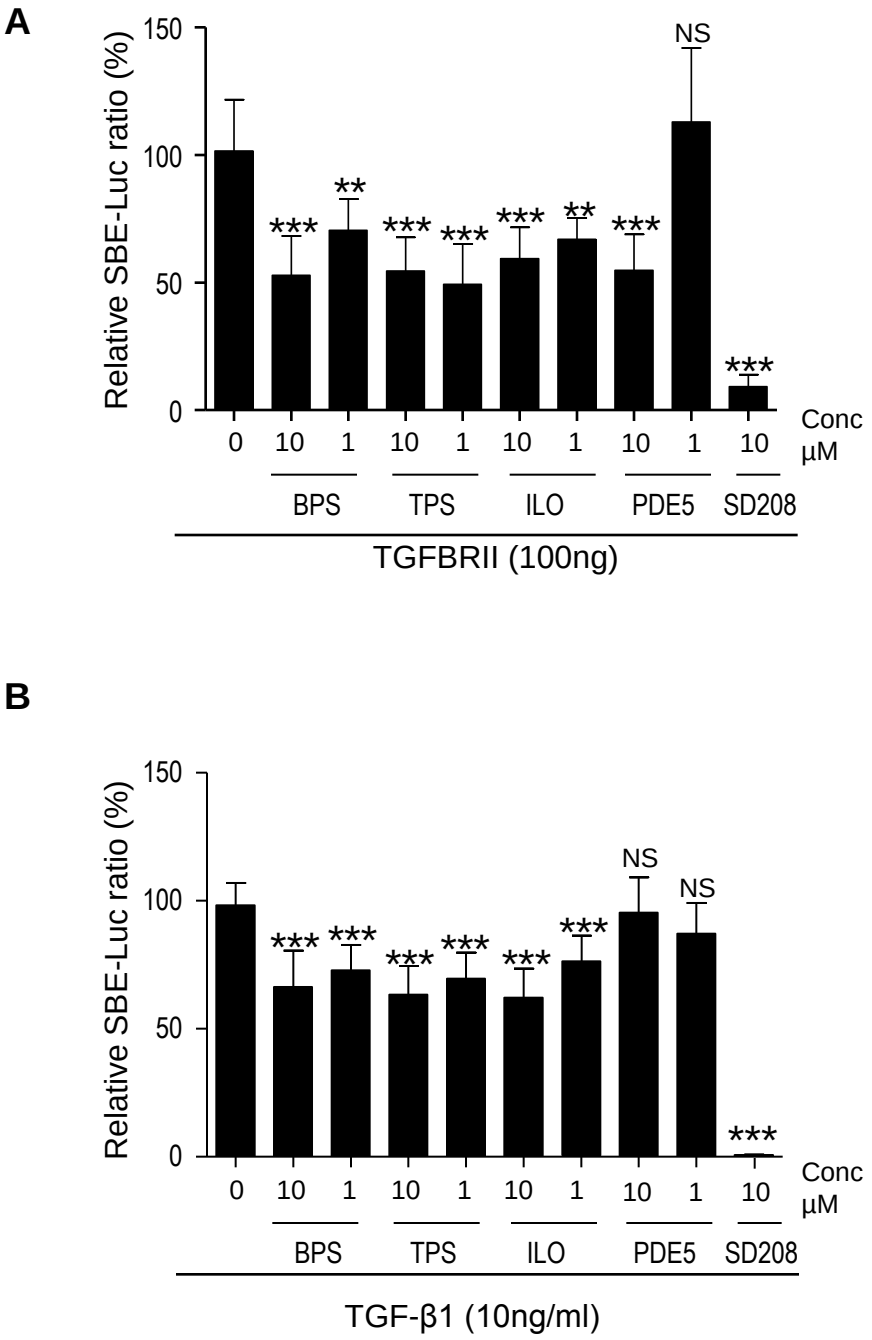
A
Relative SBE-Luc ratio (%)
150
100
50
0
NS
***
**
***
***
***
**
***
***
0
10
1
10
1
10
1
10
1
10
Conc
μM
BPS
TPS
ILO
PDE5
SD208
TGFBRII (100ng)
B
Relative SBE-Luc ratio (%)
150
100
50
0
NS
NS
***
***
***
***
***
***
***
0
10
1
10
1
10
1
10
1
10
Conc
μM
BPS
TPS
ILO
PDE5
SD208
TGF-β1 (10ng/ml)

Figure 5

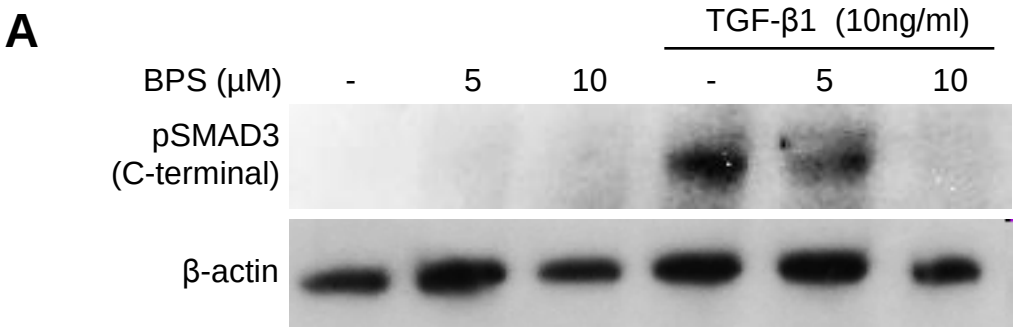
A
TGF-β1 (10ng/ml)
BPS (μM) - 5 10 - 5 10
pSMAD3
(C-terminal)
β-actin

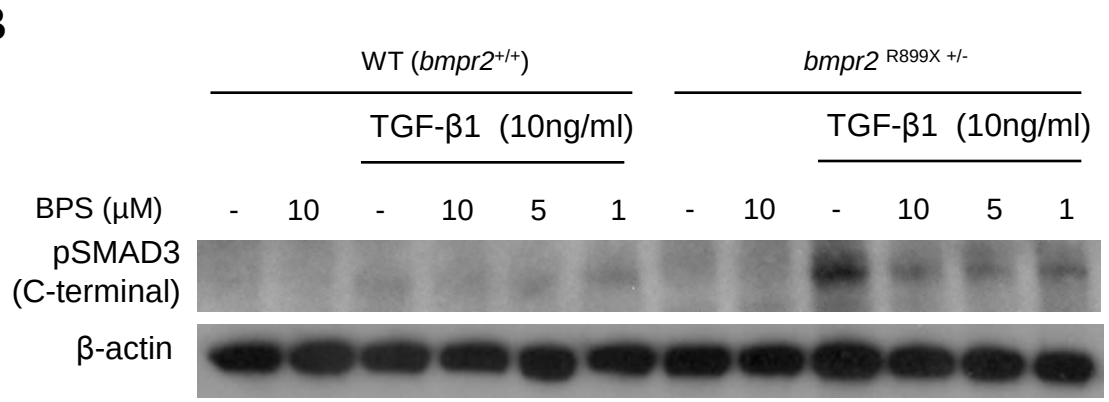
B
WT (bmpr2+/+)
bmpr2 R899X +/-
TGF-β1 (10ng/ml)
TGF-β1 (10ng/ml)
BPS (μM) - 10 - 10 5 1 - 10 - 10 5 1
pSMAD3
(C-terminal)
β-actin

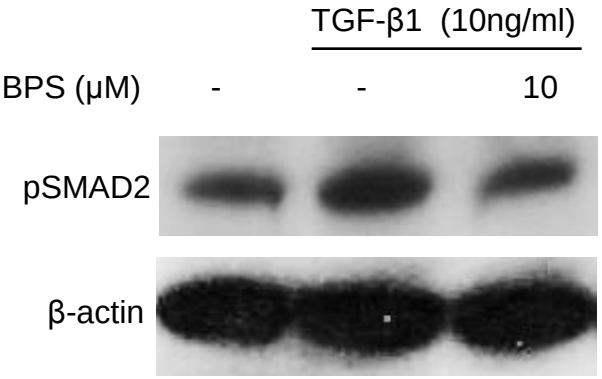
D
TGF-β1 (10ng/ml)
BPS (μM) - - 10
pSMAD2
β-actin

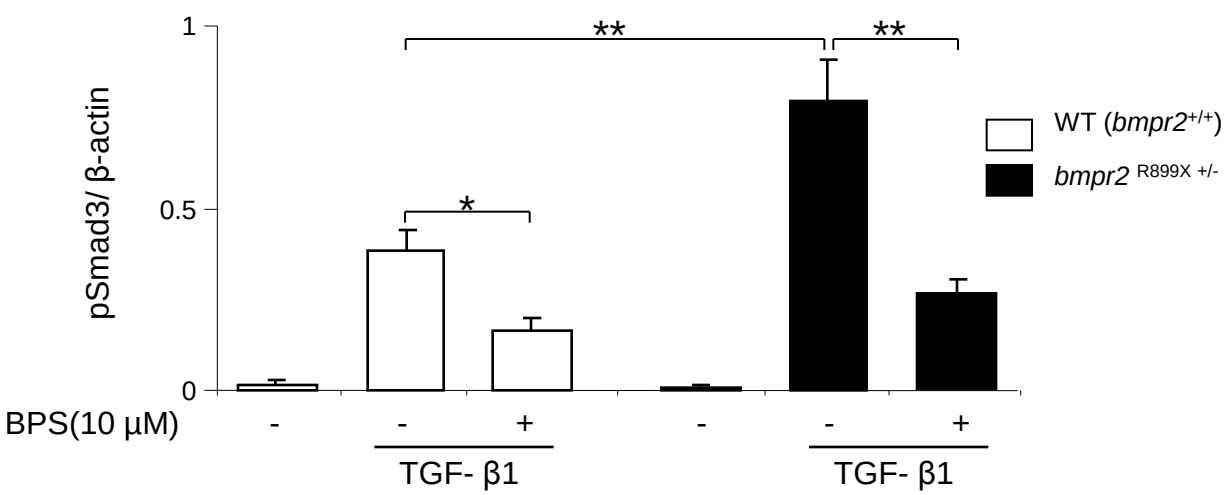
C
pSmad3/ β-actin
1
0.5
0
**
**
*
WT (bmpr2+/+)
bmpr2 R899X +/-
BPS(10 μM) - - + - - +
TGF- β1
TGF- β1

Figure 6

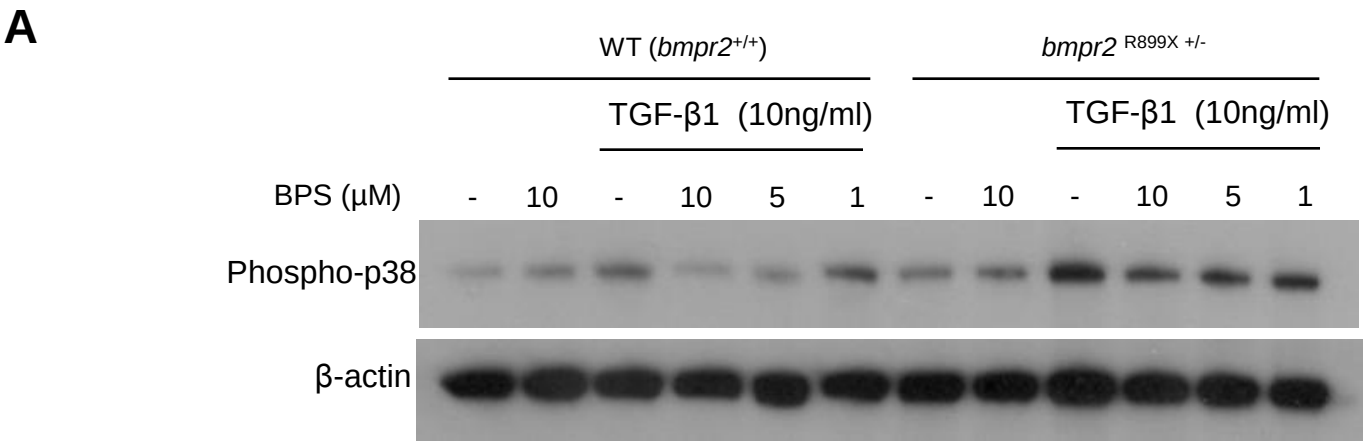
A
WT (bmpr2+/+)
bmpr2 R899X +/-
TGF-β1 (10ng/ml)
TGF-β1 (10ng/ml)
BPS (μM) - 10 - 10 5 1 - 10 - 10 5 1
Phospho-p38
β-actin

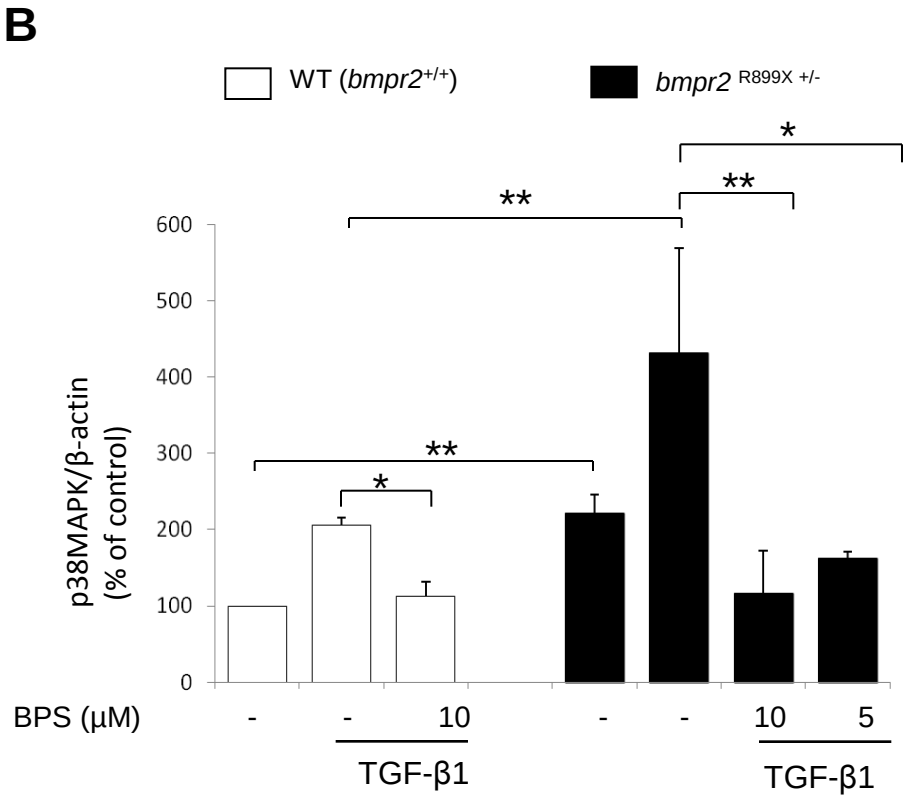
B
WT (bmpr2+/+)
bmpr2 R899X +/-
p38MAPK/β-actin (% of control)
600
500
400
300
200
100
0
**
**
*
**
*
BPS (μM) - - 10 - - 10 5
TGF-β1
TGF-β1

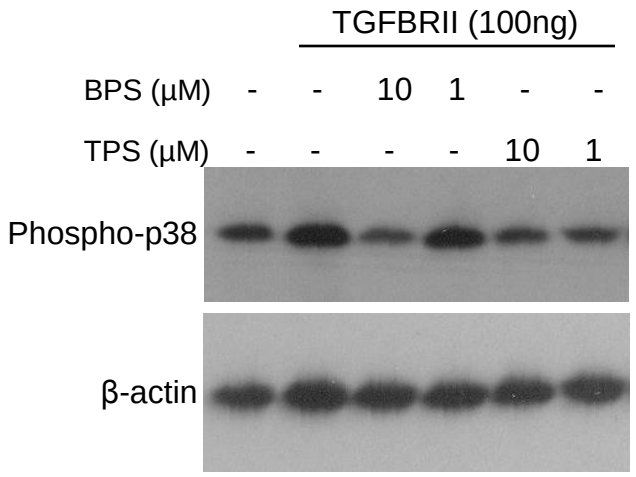
C
TGFBRII (100ng)
BPS (μM) - - 10 1 - -
TPS (μM) - - - - 10 1
Phospho-p38
β-actin

Figure 7

A

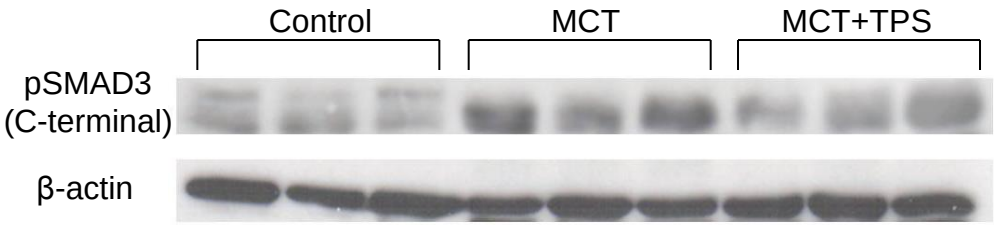
Control
MCT
MCT+TPS
pSMAD3
(C-terminal)
β-actin

B

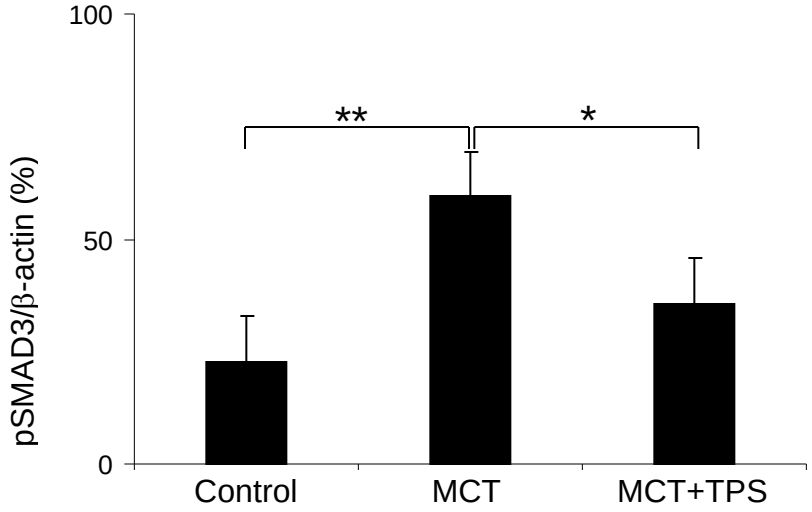
100
50
0
pSMAD3/β-actin (%)
**
*
Control
MCT
MCT+TPS

C

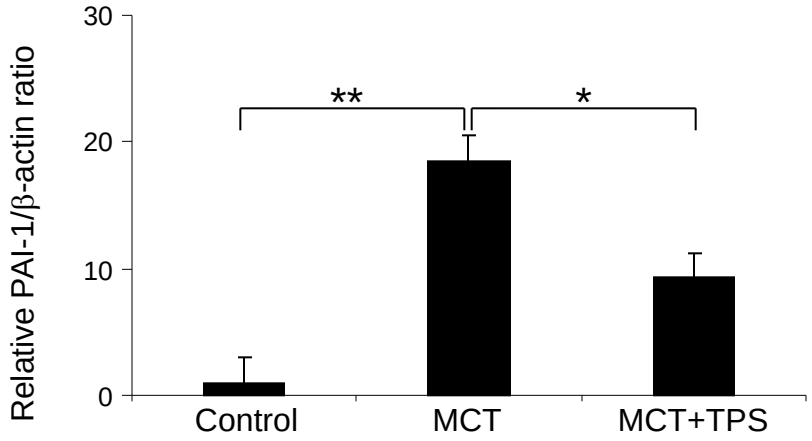
30
20
10
0
Relative PAI-1/β-actin ratio
**
*
Control
MCT
MCT+TPS